Research Article | Vol. 7, No. 3 | 1 Mar 2017 | OPTICAL MATERIALS EXPRESS 698
Optical Materials EXPRESS

Mid-infrared astrophotonics: study of ultrafast laser induced index change in compatible materials

A. Arriola,[1,2,*] S. Gross,[1,2] M. Ams,[1,2] T. Gretzinger,[1,2] D. Le Coq,[3] R. P. Wang,[2,4,5] H. Ebendorff-Heidepriem,[6] J. Sanghera,[7] S. Bayya,[7] L. B. Shaw,[7] M. Ireland,[8] P. Tuthill,[9] and M. J. Withford[1,2]

[1]*MQ Photonics Research Centre, Department of Physics and Astronomy, Macquarie University, Australia*
[2]*Centre for Ultrahigh bandwidth Devices for Optical Systems (CUDOS), Australia*
[3]*Institut des Sciences Chimiques de Rennes, Eq. Verres et Ceramiques, UMR 6226 CNRS, Univ. Rennes 1, 35042 Rennes Cedex, France*
[4]*Laboratory of Infrared Materials and Devices, Institute for Advanced Studies, Ningbo University, Ningbo 315211, China*
[5]*Laser Physics Centre, Research School of Physics and Engineering, Australian National University, Canberra, Australia*
[6]*ARC Centre of Excellence for Nanoscale BioPhotonics, Institute for Photonics and Advanced Sensing and School of Physical Sciences, University of Adelaide, Australia*
[7]*US Naval Research Laboratory, Code 5623, 4555 Overlook Ave., SW, Washington, DC 20375, USA*
[8]*Research School of Astronomy and Astrophysics, Australian National University, Canberra, Australia*
[9]*Sydney Institute for Astronomy (SIfA), School of Physics, University of Sydney, Australia*
[*]*alex.arriola@mq.edu.au*

Abstract: The mid-infrared wavelength regime 3.5 – 4.1μm, known as the astronomical L' band is of special interest for exoplanet hunting. Mid-IR compatible photonic technologies are an enabling platform for a range of critical observational science using compact instruments on the next generation of Extremely Large Telescopes. Pupil remapping interferometry is a technique in which subapertures of the telescope pupil (2D) are reformatted into a 1D linear array. This can be done efficiently using 3D photonics. One of the most important techniques to fabricate 3D photonic devices in glass is ultrafast laser inscription. However, common silicate glasses are opaque above 2-2.2 μm and therefore not useful for the fabrication of waveguides at mid-infrared wavelengths. Here we present a study of mid-infrared transparent materials that are compatible with the ultrafast laser inscription technique. This study will inform the development of mid-infrared photonic devices for future exoplanetary discovery.

OCIS codes: (130.2755) Glass waveguides; (130.3060) Infrared; (140.3390) Laser materials processing; (220.4000) Microstructure fabrication; (350.1260) Astronomical optics; (350.1270) Astronomy and astrophysics.

References and links

1. L. Labadie and O. Wallner, "Mid-infrared guided optics: a perspective for astronomical instruments," Opt. Express **17**, 1947-1962 (2009).
2. N. Madhusudhan, A. Burrows, and T. Currie, "Model Atmospheres for Massive Gas Giants With Thick Clouds: Application To the Hr 8799 Planets and Predictions for Future Detections," Astrophys. J. **737**, 34 (2011).
3. F. Malbet, P. Kern, I. Schanen-Duport, J. P. Berger, and K. Rousselet-Perraut, "Integrated optics for astronomical interferometry. I. Concept and astronomical applications," Astron. Astrophys. Supp. Series **145**, 135 (1999).
4. R. R. Thomson, R. J. Harris, T. A. Birks, and G. Brown, "Ultrafast Laser Inscription of a 121-Waveguide Fan-Out for Astrophotonics," Opt. Lett. **37**, 2331–2333 (2006).
5. S. G. Leon-Saval, A. Argyros, and J. Bland-Hawthorn, "Photonic lanterns," Nanophotonics **2**, 429–440 (2013).
6. N. Jovanovic, S. Gross, C. Miese, A. Fuerbach, J. Lawrence, and M. J. Withford, "Direct laser written multimode waveguides for astronomical applications," in "Proceedings of SPIE **7739**" (2010).
7. A. Arriola, S. Gross, N. Jovanovic, N. Charles, P. G. Tuthill, S. M. Olaizola, A. Fuerbach, and M. J. Withford, "Low bend loss waveguides enable compact, efficient 3D photonic chips," Opt. Express **21**, 2978–2986 (2013).

#282946 https://doi.org/10.1364/OME.7.000698
Journal © 2017 Received 15 Dec 2016; revised 24 Jan 2017; accepted 24 Jan 2017; published 2 Feb 2017

Optical Materials EXPRESS

8. S. Gross and M. J. Withford, "Ultrafast-laser-inscribed 3D integrated photonics: challenges and emerging applications," Nanophotonics **4**, 332–352 (2015).
9. F. Eisenhauer, G. Perrin, W. Brandner, C. Straubmeier, A. Richichi, S. Gillessen, J.-P. Berger, S. Hippler, A. Eckart, M. Schöller, S. Rabien, F. Cassaing, R. Lenzen, M. Thiel, Y. Clénet, J. R. Ramos, S. Kellner, P. Fédou, H. Baumeister, R. Hofmann, E. Gendron, A. Boehm, H. Bartko, X. Haubois, R. Klein, K. Dodds-Eden, K. Houairi, F. Hormuth, A. Gräter, L. Jocou, V. Naranjo, R. Genzel, P. Kervella, T. Henning, N. Hamaus, S. Lacour, U. Neumann, M. Haug, F. Malbet, W. Laun, J. Kolmeder, T. Paumard, R.-R. Rohloff, O. Pfuhl, K. Perraut, J. Ziegleder, D. Rouan, and G. Rousset, "GRAVITY: getting to the event horizon of Sgr A*," in "SPIE: Optical and Infrared Interferometry," **7013**, 70132 (2008).
10. A. Arriola, B. Norris, N. Cvetojevic, S. Gross, J. Lawrence, M. Withford, and P. Tuthill, "First on-sky demonstration of a compact fully-integrated Photonic Waveguide Nulling Interferometer," in "CLEO: Symposium on Advances and Opportunities in Astrophotonics II" (2016).
11. J. Bland-Hawthorn and P. Kern, "Astrophotonics: a new era for astronomical instruments," Opt. Express **17**, 1880–1884 (2009).
12. J. P. Berger, K. Rousselet-Perraut, P. Kern, F. Malbet, I. Schanen-Duport, F. Reynaud, P. Haguenauer, and P. Benech, "Integrated optics for astronomical interferometry. II. First laboratory white-light interferograms," Astron. Astrophys. Supplement Series **139**, 173–177 (1999).
13. A. Arriola, S. Mukherjee, D. Choudhury, L. Labadie, and R. R. Thomson, "Ultrafast laser inscription of mid-IR directional couplers for stellar interferometry," Opt. Lett. **39**, 4823–4822 (2014).
14. S. Gross, N. Jovanovic, A. Sharp, M. Ireland, J. Lawrence, and M. J. Withford, "Low loss mid-infrared ZBLAN waveguides for future astronomical applications," Opt. Express **23**, 7946 (2015).
15. M. Benisty, J.-P. Berger, L. Jocou, P. Labeye, F. Malbet, K. Perraut, and P. Kern, "An integrated optics beam combiner for the secondÃŁgeneration VLTI instruments," Astron. Astrophys. **498**, 601–613 (2009).
16. C. Hanot, B. Mennesson, S. Martin, K. Liewer, F. Loya, D. Mawet, P. Riaud, O. Absil, and E. Serabyn, "Improving interferometric null depth measurements using statistical distributions : theory and first results with the Palomar Fiber Nuller," Astrophys. J. **729**, 110 (2011).
17. E. Huby, G. Perrin, F. Marchis, S. Lacour, T. Kotani, G. Duchêne, E. Choquet, E. L. Gates, J. M. Woillez, O. Lai, P. Fédou, C. Collin, F. Chapron, V. Arslanyan, and K. J. Burns, "Astrophysics FIRST , a fibered aperture masking instrument I . First on-sky test results," Astron. Astrophys. **A55** (2012).
18. N. Cvetojevic, J. S. Lawrence, S. C. Ellis, and R. Haynes, "Characterization and on-sky demonstration of an integrated photonic spectrograph for astronomy," Opt. Express **17**, 1060–1065 (2009).
19. B. Barnaby, N. Cvetojevic, S. Gross, P. N. Stewart, N. Charles, J. S. Lawrence, M. J. Withford and P. Tuthill, "High-performance 3D waveguide architecture for astronomical pupil-remapping interferometry," Opt. Express **22**, 18335-18353 (2014).
20. K. M. Davis, K. Miura, N. Sugimoto, and K. Hirao, "Writing waveguides in glass with a femtosecond laser," Opt. Lett. **21**, 1729–1731 (1996).
21. K. Miura, J. Qiu, H. Inouye, T. Mitsuyu, and K. Hirao, "Photowritten optical waveguides in various glasses with ultrashort pulse laser," Appl. Phys. Lett. **71**, 3329 (1997).
22. R. Osellame, V. Maselli, N. Chiodo, D. Polli, R. M. Vazquez, R. Ramponi, and G. Cerullo, "Fabrication of 3D photonic devices at 1.55 um wavelength by femtosecond Ti:Sapphire oscillator," Electron. Lett. **41**, 315–317 (2005).
23. S. M. Eaton, W. Chen, L. Zhang, H. Zhang, R. Iyer, J. S. Aitchison, and P. R. Herman, "Telecom-Band Directional Coupler Written With Femtosecond Fiber Laser," IEEE Photon. Technol. Lett. **18**, 2174–2176 (2006).
24. S. Gross, M. Ams, G. Palmer, C. T. Miese, R. J. Williams, G. D. Marshall, A. Fuerbach, D. G. Lancaster, H. Ebendorff-Heidepriem, and M. J. Withford, "Ultrafast Laser Inscription in Soft Glasses: A Comparative Study of Athermal and Thermal Processing Regimes for Guided Wave Optics," Int. J. Appl. Glass Sci. **3**, 332–348 (2012).
25. J.-P. Bérubé, M. Bernier, and R. Vallée, "Femtosecond laser-induced refractive index modifications in fluoride glass," Opt. Mater. Express **3**, 598–611 (2013).
26. J. Hu, J. Meyer, K. Richardson, and L. Shah, "Feature issue introduction: mid-IR photonic materials," Opt. Mater. Express **3**, 1571 (2013).
27. B. Bureau, X. H. Zhang, F. Smektala, J.-L. Adam, J. Troles, H.-l. Ma, C. Boussard-Plèdel, J. Lucas, P. Lucas, D. Le Coq, M. R. Riley, and J. H. Simmons, "Recent advances in chalcogenide glasses," J. Non-Cryst. Solids **345-346**, 276–283 (2004).
28. K. Richardson, D. Krol, and K. Hirao, "Glasses for Photonic Applications," Int. J. Appl. Glass Sci. **1**, 74–86 (2010).
29. J. M. Parker, "Fluoride Glasses," Annu. Rev. Mater. Sci. **19**, 21–41 (1989).
30. J. Martínez, A. Ródenas, T. Fernandez, J. R. Vázquez de Aldana, R. R. Thomson, M. Aguiló, A. K. Kar, J. Solis, and F. Díaz, "3D laser-written silica glass step-index high-contrast waveguides for the 3.5um mid-infrared range," Opt. Lett. **40**, 5818–5821 (2015).
31. K. Tanaka, "Photoexpansion in As_2S_3 glass," Phys. Rev. B **57**, 5163–5167 (1998).
32. N. Carlie, N. C. Anheier, H. a. Qiao, B. Bernacki, M. C. Phillips, L. Petit, J. D. Musgraves, and K. Richardson, "Measurement of the refractive index dispersion of As2Se3 bulk glass and thin films prior to and after laser irradiation and annealing using prism coupling in the near- and mid-infrared spectral range," Rev. Sci. Instrum. **82**, 053103 (2011).
33. R. A. Nyquist and R. O. Kagel, *Handbook of Infrared and Raman Spectra of Inorganic Compounds and Organic*

Optical Materials EXPRESS

Salts: Infrared Spectra of Inorganic Compounds (Academic Press, 2012).
34. E. Poppe, B. Srinivasan, and R. Jain, "980 nm diode-pumped continuous wave mid-IR (2.7 Âţm) fibre laser," Electron. Lett. **34**, 2331–2333 (1998).
35. G. Tao, H. Ebendorff-Heidepriem, A. M. Stolyarov, S. Danto, J. V. Badding, Y. Fink, J. Ballato, and A. F. Abouraddy, "Infrared Fibers," Adv. Opt. Photonics **7**, 379–458 (2015).
36. B. J. Eggleton, B. Luther-Davies, and K. Richardson, "Chalcogenide photonics," Nat. Photon. **5**, 725–725 (2011).
37. K. Tanaka, "Spectral dependence of photoexpansion in As_2S_3 glass," Philos. Mag. Lett. **79**, 25–30 (1999).
38. O. Efimov, L. Glebov, K. Richardson, E. Van Stryland, T. Cardinal, S. Park, M. Couzi, and J. Brunéel, "Waveguide writing in chalcogenide glasses by a train of femtosecond laser pulses," Opt. Mater. **17**, 379–386 (2001).
39. A. Zoubir, M. Richardson, C. Rivero, A. Schulte, C. Lopez, K. Richardson, N. Hô, and R. Vallée, "Direct femtosecond laser writing of waveguides in As2S3 thin films," Opt. Lett. **29**, 748–750 (2004).
40. C. Lopez, K. Richardson, a. Zoubir, M. Richardson, a. Schulte, and a. Pope, "Photo-induced optical and physical property modifications in chalcogenide thin films by femtosecond irradiation," (CLEO). Conference on Lasers and Electro-Optics, 2005, pp. 74–76, Vol. 1 (2005).
41. D.-Y. Choi, S. Madden, D. Bulla, R. Wang, A. Rode, and B. Luther-Davies, "Thermal annealing of arsenic tri-sulphide thin film and its influence on device performance," J. Appl. Phys. **107**, 053106 (2010).
42. M. Dussauze, X. Zheng, V. Rodriguez, E. Fargin, T. Cardinal, and F. Smektala, "Photosensitivity and second harmonic generation in chalcogenide arsenic sulfide poled glasses," Opt. Mater. Express **2**, 45–54 (2011).
43. O. Caulier, D. Le Coq, E. Bychkov, and P. Masselin, "Direct laser writing of buried waveguide in As_2S_3 glass using a helical sample translation," Opt. Lett. **38**, 4212–4215 (2013).
44. C. D'Amico, G. Cheng, C. Mauclair, J. Troles, L. Calvez, V. Nazabal, C. Caillaud, G. Martin, B. Arezki, E. LeCoarer, P. Kern, and R. Stoian, "Large-mode-area infrared guiding in ultrafast laser written waveguides in Sulfur-based chalcogenide glasses," Opt. Express **22**, 13091–13101 (2014).
45. L. Calvez, Z. Yang, and P. Lucas, "Light-Induced Matrix Softening of Ge-As-Se Network Glasses," Phys. Rev. Lett. **101**, 177402 (2008).
46. L. Calvez, Z. Yang, and P. Lucas, "Composition dependence and reversibility of photoinduced refractive index changes in chalcogenide glass," J. Phys. D: Appl. Phys. **43**, 445401 (2010).
47. R. P. Wang, *Amorphous Chalcogenides: Advances and Applications* (Pan Stanford Publishing, 2014).
48. E. Romanova, A. Konyukhov, S. Muraviov, and A. Andrianov, "Thermal diffusion in chalcogenide glass irradiated by a train of femtosecond laser pulses," 2010 12th International Conference on Transparent Optical Networks, ICTON 2010 pp. 26–29 (2010).
49. S. Messaddeq, J. Bérubé, M. Bernier, I. Skripachev, R. Vallée, and Y. Messaddeq, "Thermal diffusion in chalcogenide glass irradiated by a train of femtosecond laser pulses," Opt. Express **20**, 1–4 (2012).
50. J. P. Bérubé, S. H. Messaddeq, M. Bernier, I. Skripachev, Y. Messaddeq, and R. Vallée, "Tailoring the refractive index of Ge-S based glass for 3D embedded waveguides operating in the mid-IR region," Opt. Express **22**, 26103–26116 (2014).
51. C. D'Amico, C. Caillaud, P. K. Velpula, M. K. Bhuyan, M. Somayaji, J. Troles, L. Calvez, V. Nazabal, A. Boukenter, R. Stoian, L. H. Curien, U. M. R. Cnrs, U. D. Lyon, U. J. Monnet, and S. Etienne, "Ultrafast laser-induced refractive index changes in Ge15As15S70 chalcogenide glass," Opt. Mater. Express **6**, 1914–1928 (2016).
52. T. Schweizer, D. Hewak, B. Samson, and D. Payne, "Spectroscopy of potential mid-infrared laser transitions in gallium lanthanum sulphide glass," J. Lumin. **419**, 72–74 (1997).
53. P. Masselin, D. Coq, L. Calvez, E. Petracovschi, E. Lépine, E. Bychkov, and X. Zhang, "CsCl effect on the optical properties of the $80GeS_2$-$20Ga_2S_3$ base glass," Appl. Phys. A **106**, 697–702 (2011).
54. D. W. Hewak, D. Brady, R. J. Curry, G. Elliott, C.-c. Huang, M. Hughes, K. Knight, A. Mairaj, M. Petrovich, R. Simpson, C. Smith, and C. Sproat, "Chalcogenide Glasses for Photonics Device Applications With contributions from," Tech. rep., Optoelectronics Research Centre, University of Southampton (UK), Southampton (2008).
55. P. Masselin, E. Bychkov, and D. Le Coq, "Direct laser writing of a low-loss waveguide with independent control over the transverse dimension and the refractive index contrast between the core and the cladding," Opt. Lett. **41**, 3507–3510 (2016).
56. M. Hughes, W. Yang, and D. Hewak, "Fabrication and characterization of femtosecond laser written waveguides in chalcogenide glass," Appl. Phys. Lett. **90**, 131113 (2007).
57. N. D. Psaila, R. R. Thomson, H. T. Bookey, S. Shen, N. Chiodo, R. Osellame, G. Cerullo, A. Jha, and A. K. Kar, "Supercontinuum generation in an ultrafast laser inscribed chalcogenide glass waveguide," Opt. Express **15**, 15776–15781 (2007).
58. B. McMillen, B. Zhang, K. P. Chen, A. Benayas, and D. Jaque, "Ultrafast laser fabrication of low-loss waveguides in chalcogenide glass with 0.65 dB/cm loss," Opt. Lett. **37**, 1418–1420 (2012).
59. J. E. McCarthy, H. T. Bookey, N. D. Psaila, R. R. Thomson, and A. K. Kar, "Mid-infrared spectral broadening in an ultrafast laser inscribed gallium lanthanum sulphide waveguide," Opt. Express **20**, 1545–1551 (2012).
60. A. Ródenas, G. Martin, B. Arezki, N. Psaila, G. Jose, A. Jha, L. Labadie, P. Kern, A. Kar, and R. Thomson, "Three-dimensional mid-infrared photonic circuits in chalcogenide glass," Opt. Lett. **37**, 392–394 (2012).
61. X. Liu, W. Zhang, W. Zhao, R. Stoian, and G. Cheng, "Expanded-core waveguides written by femtosecond laser irradiation in bulk optical glasses," Opt. Express **22**, 28771–28782 (2014).
62. T. Gretzinger, S. Gross, M. Ams, A. Arriola, and M. J. Withford, "Ultrafast laser inscription in chalcogenide glass:

Optical Materials EXPRESS

thermal versus athermal fabrication," Opt. Mater. Express **5**, 2862–2877 (2015).
63. A. Arriola, D. Choudhury, and R. R. Thomson, "Towards efficient mid-infrared integrated photonic-lanterns," J. Opt. **17**, 125804 (2015).
64. G. Demetriou, J.-P. Bérubé, R. Vallée, Y. Messaddeq, C. R. Petersen, D. Jain, O. Bang, C. Craig, D. W. Hewak, and A. K. Kar, "Refractive index and dispersion control of ultrafast laser inscribed waveguides in gallium lanthanum sulphide for near and mid-infrared applications," Opt. Express **24**, 6350–6358 (2016).
65. T. Anderson, N. Carlie, L. Petit, J. Hu, a. Agarwal, J. Viens, J. Choi, L. Kimmerling, K. Richardson, and M. Richardson, "Refractive index modifications in Chalcogenide films induced by sub-bandgap near-IR femtosecond pulses," 2007 Conference on Lasers and Electro-Optics (CLEO) pp. 1–2 (2007).
66. B. E. A. Saleh and M. C. Teich, *Fundamentals of Photonics* (Wiley & Sons, 2007), second ed.
67. J. Bei, T. M. Monro, A. Hemming, and H. Ebendorff-Heidepriem, "Fabrication of extruded fluoroindate optical fibers," Opt. Mater. Express **3**, 318 (2013).
68. C. W. Ponader, J. F. Schroeder, and A. M. Streltsov, "Origin of the refractive-index increase in laser-written waveguides in glasses," J. Appl. Phys. **103** (2008).
69. D. J. Little, M. Ams, S. Gross, P. Dekker, C. T. Miese, A. Fuerbach, and M. J. Withford, "Structural changes in BK7 glass upon exposure to femtosecond laser pulses," J. Raman Spectrosc. **42**, 715–718 (2011).
70. V. R. Bhardwaj, P. B. Corkum, D. M. Rayner, C. Hnatovsky, E. Simova, and R. S. Taylor, "Stress in femtosecond-laser-written waveguides in fused silica," Opt. Lett. **29**, 1312–1314 (2004).
71. D. Rayner, a. Naumov, and P. Corkum, "Ultrashort pulse non-linear optical absorption in transparent media," Opt. Express **13**, 3208–3217 (2005).
72. T. T. Fernandez, M. Hernandez, B. Sotillo, S. M. Eaton, G. Jose, R. Osellame, A. Jha, P. Fernandez, and J. Solis, "Role of ion migrations in ultrafast laser written tellurite glass waveguides." Opt. Express **22**, 15298–15304 (2014).
73. S. Gross, M. Dubov, and M. J. Withford, "On the use of the Type I and II scheme for classifying ultrafast laser direct-write photonics," Opt. Express **23**, 7767 (2015).
74. Y. Nasu, M. Kohtoku, and Y. Hibino, "Low-loss waveguides written with a femtosecond laser for flexible interconnection in a planar light-wave circuit," Opt. Lett. **30**, 723–725 (2005).
75. R. Stoian, C. D. Amico, M. K. Bhuyan, and G. Cheng, "Ultrafast laser photoinscription of large-mode-area waveguiding structures in bulk dielectrics," Opt. and Laser Technol. **80**, 98–103 (2016).
76. S. Gross, M. Ams, D. G. Lancaster, T. M. Monro, A. Fuerbach, and M. J. Withford, "Femtosecond direct-write uberstructure waveguide Bragg gratings in ZBLAN," Opt. Lett. **37**, 3999–4001 (2012).
77. R. Graf, A. Fernandez, M. Dubov, H. J. Brueckner, B. N. Chichkov, and A. Apolonski, "Pearl-chain waveguides written at megahertz repetition rate," Appl. Phys. B **87**, 21–27 (2007).
78. D. Marcuse, "Loss Analysis of Single Mode Fiber Splices," Bell Syst. Tech. J. **56**, 703–718 (1977).
79. K. Petermann, "Fundamental mode microbending loss in graded-index and W fibres," Opt. Quant. Electron. **9**, 167–175 (1977).
80. D. G. Lancaster, S. Gross, A. Fuerbach, H. E. Heidepriem, T. M. Monro, and M. J. Withford, "Versatile large-mode-area femtosecond laser-written Tm:ZBLAN glass chip lasers," Opt. Express **20**, 27503–27509 (2012).

1. Introduction

The mid-infrared (MIR), 5-20 μm, represents a fascinating wavelength range for astronomy for a variety of reasons, particularly for exoplanet hunting. Celestial objects emit infrared radiation at wavelengths strongly related to their temperature [1]. Relatively warm objects (> 300 K) such as the Earth are much brighter in the wavelength region known as the astronomical L' band ($3.5 - 4.1\mu$m) than in the near-infrared. At the same time, the brightness of the host star is generally still rising to peak at much shorter wavelengths (often in the visible). As a consequence, the brightness contrast between the star and planet presents a less daunting observational challege in the L' band [2]. In addition, the mid-IR comprises the "chemical fingerprint" region, where biomarkers such as water, methane and carbon dioxide can be found through their spectroscopic bands.

Research projects and publications during the last decade [3–8] have demonstrated that photonic devices can greatly simplify ground-based and space-borne astronomical instruments and improve their performance [9, 10]. These findings facilitated the birth of a new research discipline: termed *astrophotonics* [11], where photonic technologies are expected to have an important role in the next generation of Extremely Large Telescopes (ELTs) [1] due to the ability to integrate components such as beam combiners [12–17] and spectrographs [18] in palm-size devices. Their small size makes them easy to temperature stabilise and to implement within the limited instrument volumes available in current telescope facilities. Interferometry is one of the

Optical Materials EXPRESS

main applications of astrophotonics, however it requires reformatting the telescope pupil (2D) into a linear 1D array of single mode waveguides before recombining them for interferometric processing. This reformatting needs a 3D device configuration based on optical fibres or arrays of 3D waveguides. The latter option adds robustness to the system and makes it more insensitive to the environment. However, one of the most mature fabrication techniques for optical waveguides, *lithography*, is poorly suited to the creation of arbitrary 3D configurations that not only reformat the pupil the pupil plane of a telescope but do so via a set of waveguides that share the same optical path length in order to preserve the spatial coherence of the guided wave. More details about the design requirements of these reformatting devices can be found in [19]. A leading technology that offers the possibility to fabricate full 3D, compact photonic components is ultrafast laser inscription (ULI) [20]. Over the last two decades there has been a lot of research on the interaction between femtosecond laser pulses and transparent glasses (silicates [21–23], phosphates [24], fluorides [25], etc) to fabricate waveguides tailored for different wavelengths and applications. However, the transparency of common silica glasses rapidly decays beyond 2-2.2 μm. In order to achieve good transparency at longer wavelengths exotic materials (i.e. chalcogenides, fluorides, etc) are required (featured in a special journal issue [26]). This class of glasses presents new challenges that stem from their properties such as large nonlinearities [27], brittleness and sensitivity to UV radiation or hygroscopicity [28]. Nonlinearities, for example, exponentially increase from the fluoride family of glasses [29], to oxides [30], sulfides [31] and selenides [32]. The ultrafast laser inscription of waveguides requires high peak power pulses in order to modify the material at the focal volume. The high nonlinearities of these materials can distort the beam and change the focusing conditions of the femtosecond laser beam during the inscription process.

Fluorides [29] are a family of materials based on fluorine as the main component and can range from a two element crystal such as CaF_2 [33] to more complicated multicomponent compositions like ZBLAN (ZrF_4-BaF_2-LaF_3-AlF_3-NaF) [14, 34, 35]. They benefit from their low refractive index (around 1.5), which reduces the influence of spherical aberrations during ULI, avoids the requirement for complicated multilayer antireflection coatings as can be the case for chalcogenides, whose refractive index is usually above 2 [14].

Chalcogenide glasses represent an important class of amorphous semiconductor consisting of at least one or more of the chalcogen elements: sulphur, selenium and tellurium [36]. These elements are covalently bonded to network former such as As, Ge, Sb, Ga, Si or P [36] enabling a wide variety of possible stoichiometries.

Early work on femtosecond laser inscription in chalcogenides started with the simplest forms of glass: arsenic selenides (As_2Se_3) [32] and arsenic sulphides As_2S_3 [21, 31, 37–44], the latter glass featuring the lowest nonlinearity by an order of magnitude among the chalcogenide glasses. This makes sulphides in general more suitable when tightly focusing ultrashort laser pulses. The majority of these glasses produce a negative refractive index when exposed to a femtosecond laser. Adding a controlled amount of germanium to these chalcogenide glasses tailors the refractive index and can change the coordination number of the glass, and tune physical properties such as photodarkening, the cut-off wavelength or density of the glass [45–47]. Moreover, the inclusion of Germanium to form Ge-As-S glasses has been shown to have an effect on the sign and magnitude of the refractive index change generated during ultrafast laser inscription [44, 48–51]. Replacing arsenic with gallium leads to a highly stable and non toxic chalcogenide glass [52–55] called Gallium Lanthanum Sulphide (GLS). GLS has become a widely studied glass due to its favourable compromise between nonlinearity and transparency [13, 56–64].

A lot of the work on femtosecond laser interaction with MIR transparent chalcogenide glasses has been done in thin films [40], bulk materials [27, 31, 32, 37, 42, 45, 46] and in waveguide fabrication [38, 39, 43, 65]. The rise in interest for the MIR over the last few years has led to elevated activity in the development of mid-IR transparent glasses [26]. Some of these glasses

Optical Materials EXPRESS

may have potential in MIR astrophotonics. Consequently it is important and timely to perform an ultrafast laser inscription parametric study of these glasses.

2. Summary of the investigated materials

For a glass to be suitable for MIR astronomical science and compatible with the ultrafast laser inscription technique for waveguide fabrication it needs to fulfil certain requirements. Firstly, the material needs to be transparent at both the MIR (~4μm) and at the inscription wavelength (800 nm, in this case), as the technique is based on nonlinear processes including multiphoton ionisation (see section 3).

Table 1. List of glasses utilised for femtosecond laser fabrication of MIR waveguides. The table also shows the type of glass and their origin. The term IZSBGC represents a family of fluoride glasses with the following fundamental chemical composition: $32InF_3$-$20ZnF_2$-SrF_2-$18BaF_2$-$8GaF_3$-$2CaF_2$.

Glass name	Type of glass	Origin
Pr : IZSBGC	Fluoride	University of Adelaide
IZSBGC	Fluoride	University of Adelaide
La : IZSBGC	Fluoride	University of Adelaide
CaF_2	Fluor. Crystal	Edmund Optics (Commercial)
$As_{39}S_{61}$	Chalcogenide	Naval Research Laboratory (USA)
$75(GeS_2)$-$15(Ga_2S_3)$-10(CsCl)	Chalcogenide	University of Rennes
$Ge_{15}Sb_{20}S_{65}$	Chalcogenide	Australian National University (ANU)
$Ge_{11.5}As_{24}S_{64.5}$	Chalcogenide	Australian National University (ANU)
$Ge_{25}As_{10}S_{65}$	Chalcogenide	Australian National University (ANU)
GLS	Chalcogenide	ChG Southampton (Commercial)
IRG-2	Germanate	Schott Glass (Commercial)

Materials with low refractive indices are preferred. This reduces the Fresnel losses at the input/output of the waveguides due to the refractive index mismatch between the glass and the air. Therefore, dielectric antireflection coatings can be avoided and a lower refractive index reduces spherical aberrations during ultrafast laser inscription. However, most of the common low refractive index glasses are not transparent in the MIR (except for fluorides), meaning that this condition may not be met. On the other hand, materials with nonlinearities as low as possible are also preferred as the distortion of the beam while being focused is directly related to the magnitude of the nonlinear refractive index of the material. Low refractive index materials also have in general low nonlinearity (see Miller's rule [66]).

Taking these restrictions into account a selection of available glasses was sourced, these listed in Table 1. All the materials are transparent at both the laser wavelength and the MIR. The term IZSBGC represents a family of fluoride glasses with the following fundamental chemical composition: $32InF_3$-$20ZnF_2$-SrF_2-$18BaF_2$-$8GaF_3$-$2CaF_2$ [67].

The transparency of the glasses was measured using a UV-VIS-NIR spectrophotometer (Cary 5000) from 175 to 3300 nm. Fig. 1 shows the absorption coefficient curve of the glasses where the Fresnel losses have already been substracted from the recorded data. The wavelength dependent Fresnel losses were calculated using the Sellmeier equation for the refractive index of the materials. The absorption coefficient determines the minimum loss for waveguides inscribed in these materials. It can be observed that in this case the absorption coefficient is well under 0.25 at long wavelengths, which is equivalent to the 1 dB/cm upper limit set for efficient astrophotonic devices. Table 2 shows the refractive index values of the studied materials at both the laser wavelength (as it can impact the inscription process) and the MIR (as it will determine the Fresnel losses at the interfaces).

Optical Materials EXPRESS

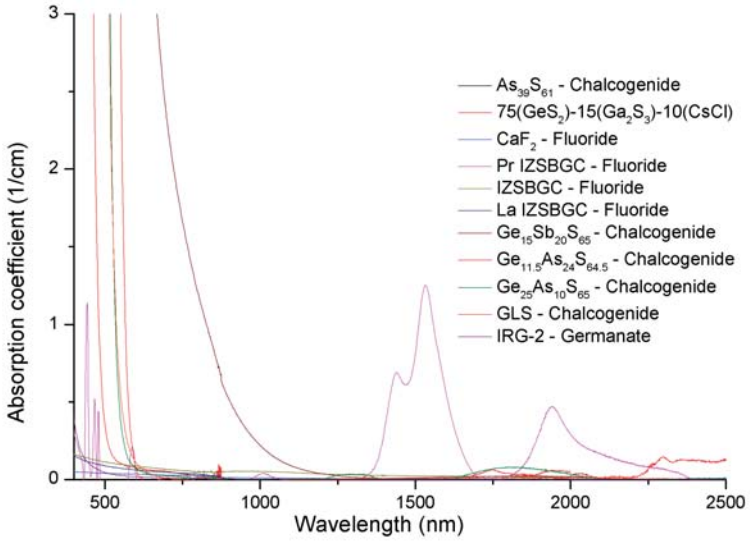

Fig. 1. Absorption coefficient curve for the selection of potential MIR glasses compatible with the ultrafast laser inscription technique.

Table 2. Refractive index value table for the selection of potential MIR glasses compatible with the ultrafast laser inscription technique..

Glass name	n (800 nm)	n (4μm)
Pr : IZSBGC	1.508	1.466
IZSBGC	1.475	1.462
La : IZSBGC	1.490	1.445
CaF_2	1.431	1.428
$As_{39}S_{61}$	2.506	2.403
$75(GeS_2)$-$15(Ga_2S_3)$-10(CsCl)	2.072	2.028
$Ge_{15}Sb_{20}S_{65}$	2.305	2.230
$Ge_{11.5}As_{24}S_{64.5}$	2.441	2.283
$Ge_{25}As_{10}S_{65}$	2.23	2.138
GLS	2.425	2.361
IRG-2	1.875	1.855

3. Fabrication

In this study, two Ti:sapphire femtosecond laser systems emitting at 800 nm were used. A regeneratively amplified, low-repetition rate femtosecond laser (Hurricane, Spectra-Physics) and an ultrafast Ti:sapphire oscillator (FEMTOSOURCE XL 500, Femtolasers GmbH). The first system produces 1 kHz pulse trains with a pulse duration of <120 fs, while the high repetition rate laser produces <50 fs pulse duration with a repetition rate of 5.1 MHz (this repetition rate can also be scaled down using a Pockel cell). The pulse duration of the lasers can be stretched to a few picoseconds by adjusting the internal compressor of the systems.

As a general rule, when fabricating waveguide structures in the low-repetition rate regime (up to a few hundred kHz) low *numerical aperture* (NA<0.6) microscope objectives were used (i.e. 20×

Optical Materials EXPRESS

Olympus UMPlanFL, NA 0.46 or 40× NA 0.6). However, when working in the high-repetition rate regime high NA microscope objectives were utilised (i.e. a.- Olympus 100× 1.25NA, b.- Zeiss N-Achroplan 100× 1.25NA and c.- Nikon 50× 0.9NA). The latter one is also known as the *thermal regime*, as opposed to the *athermal regime*, when fabricating structures at low repetition rates [62].

The refractive index change induced by the tightly focussed femtosecond pulses can be a result of one or several of the following mechanisms: densification [68, 69], stress [70], colour centres [71] or elemental diffusion [72]. This refractive index change can be positive, negative or a combination of both and the shape, sign and magnitude of this change will determine the approach taken to create a waveguide. An explanation of the different types of modifications can be found in [73]. In this paper, we present a more extensive classification of ways to create waveguides depending on specific modifications. If the refractive index modification is positive (top row of Fig. 2), the waveguide can be fabricated by inscribing a single track (P1), an overlap of modifications in the horizontal plane (P2, also known as multiscan [74]) or by grouping individual tracks around a central modification (P3). The size and magnitude of the induced refractive index will determine the overlap needed between consecutive single modification tracks. Fig. 2 shows a representation of the different modification types (and shapes) and how to create a waveguide by combining the modification tracks. This last variety can be divided into 2 kinds of waveguides depending on whether the modifications are separated or overlapped. The first version is termed expanded-core or large-mode area waveguide [44, 55, 61, 75], while the latter one will be referred as *Rosette pattern waveguide* in this manuscript. If the refractive index of the modification is negative there are 3 approaches to creating a waveguide: type I negative modifications (N1) [73], depressed cladding (N2) [76] or a combination of P2 and N2 to create a *Multiscan Depressed Cladding waveguide* (N3). In the case of N2 and N3, the overlap between modification tracks and the number of modification rings/layers around the unmodified region will determine the propagation loss properties of both the fundamental and the higher order modes. Positive refractive index modifications are usually preferred over depressed cladding structures as the fabrication times are much shorter and the design complexity of interferometric devices increases exponentially for depressed cladding waveguides. Also, depressed cladding structures are formed by many more modifications per unit area, which can lead to stress fractures.

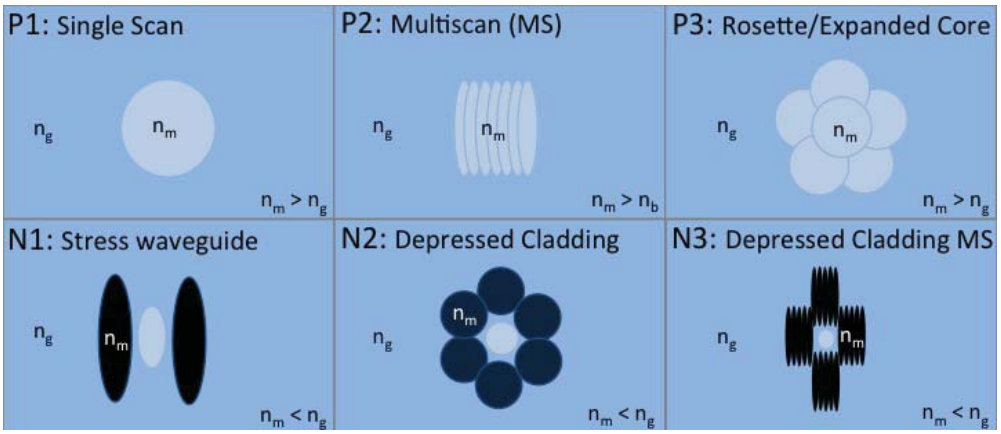

Fig. 2. Investigated waveguide geometries depending on the sign and shape of the induced refractive index change.

When analysing the tracks created in the different glasses, a wide variety of modification types can

be observed. Table 3 lists the shape and sign of the modification, together with the most suitable waveguide geometry. For some of these glasses the sign of the refractive index modification is fluence dependent. For instance the sign of refractive index change in Ge-As-S glasses can be tailored by changing the Ge/S ratio. Ge acts as a glass network former, modifying the coordination number of the glass which leads to a change in glass density and consequently to a change in refractive index of the bulk material. This phenomenon has already been shown in [44, 50]. Table 3 shows how for small concentrations of Ge, the refractive index of the modification is negative ($Ge_{11.5}As_{24}S_{64.5}$ or $Ge_{15}Sb_{20}S_{65}$), while for larger concentrations (i.e. $Ge_{25}As_{10}S_{65}$) the sign of the refractive index modification can be either positive or negative.

Table 3. Analysis of the different modification types obtained with a femtosecond laser including the shape of the modification and its sign. See Fig. 2 for a graphic representation of the suitable waveguide (wg) geometry.

Glass name	Shape of modification	Index Sign	Suitable wg Geometry
$As_{39}S_{61}$	Vertical strip	-ve	N1
75(GeS_2)-15(Ga_2S_3)-10(CsCl)	Circular	+ve	P1, P3
CaF_2	Pearl chain [77]	+ve	–
Pr : IZSBGC	Circular	+ve	P1, P3
IZSBGC	Circular	+ve	P1, P3
La : IZSBGC	Circular	+ve	P1, P3
$Ge_{15}Sb_{20}S_{65}$	Vertical strip	-ve	N1
$Ge_{11.5}As_{24}S_{64.5}$	Vertical strip	-ve	N1
$Ge_{25}As_{10}S_{65}$	Vertical strip	+ve or -ve	P1, P2, N1, N3
GLS	Tear drop	+ve	P1, P2, P3
IRG-2	Vertical Oval	-ve	N2

4. Waveguide type & morphology

As shown in the previous section, some MIR glasses exhibit a positive refractive index change while others show a negative index change when exposed to femtosecond laser radiation. This section outlines how to generate structures that support guided modes for the three material families studied: chalcogenides, fluorides and germanates.

4.1. Chalcogenides

The easiest way to inscribe a waveguide in any material using ULI occurs when the sign of the refractive index modification is positive. If, at the same time, the size and shape of the modification is proportional to the fluence applied to the glass, then fabricating waveguides at different wavelengths can be achieved by varying the irradiation conditions to obtain waveguides of the right dimensions. Unfortunately, this case does not match what happens in reality, especially with chalcogenide glasses as they present with high-nonlinearities, which result in distortion of the focused beam. This was observed, for example, during the fabrication of waveguides in GLS in the thermal regime. The shape of the modification changed from circular to a tear-drop shape when increasing the fluence. In the case of 75(GeS_2)-15(Ga_2S_3)-10(CsCl) in the thermal regime, low pulse energies were enough to fabricate round waveguides (P1) that were big enough to guide a highly confined mode at 1550 nm (MFD ~8μm) with a refractive index contrast of 7×10^{-3}, using Marcuse's equation [78, 79]. However, due to the shape dependency with the applied fluence, in order to scale up these waveguides to the MIR more complicated structures need to be built as the cross section of these modifications show regions of positive as well as negative index change. One option that can be used when the shape of a single modification

Optical Materials EXPRESS

is vertically elongated is the so-called multiscan technique (P2), where a series of tracks are overlapped horizontally to create a rectangular cross-section waveguide (see Fig. 3b). For GLS in the athermal regime, this resulted in single-mode waveguides at 1550 nm with a refractive index change of 3.5×10^{-3}. This structure could be easily scaled for guiding at longer wavelengths.

Other glasses like $As_{39}S_{61}$ and some of the Ge-As-S types are well suited to the inscription of stress waveguides (N1) in the thermal regime due to the modification shape and refractive index contrast (usually below 4×10^{-3}). $Ge_{15}Sb_{20}S_{65}$ and $Ge_{11.5}As_{24}S_{64.5}$ showed a refractive index change of around ~2-3×10^{-3}, while for $As_{39}S_{61}$ the refractive index contrast can reach up to ~4×10^{-3}. These kind of structures show strong light confinement in the horizontal axis but are relatively lossy along the vertical axis due to the lack of any refractive index change. This can be solved by adding a set of extra tracks above and below the original pair or modifications, but most of these soft glasses, because of their high thermal coefficient, suffer from stress fractures that can propagate across the whole waveguide structure. One glass well suited to this kind of structure in the athermal regime is $Ge_{25}As_{10}S_{65}$. The higher concentration of Ge (compared to the other three glasses above) is likely to improve the mechanical properties of the glass by reducing the network reticulation. This results in less mechanical stress when redensification occurs, thus reducing the susceptibility to fracture. It must be stressed that fractures can still manifest in this glass (as illustrated in Fig. 3c). This material can be used to create multiscan depressed cladding structures (N3). The refractive index contrast obtained for this chalcogenide is the largest of all these glasses (~7×10^{-3}). The multiscan depressed cladding geometry also has the benefit of straight forward scalability in size to tailor the waveguide to longer wavelengths. Fig. 3 shows three of the largest refractive indices obtained for some of the chalcogenide glasses.

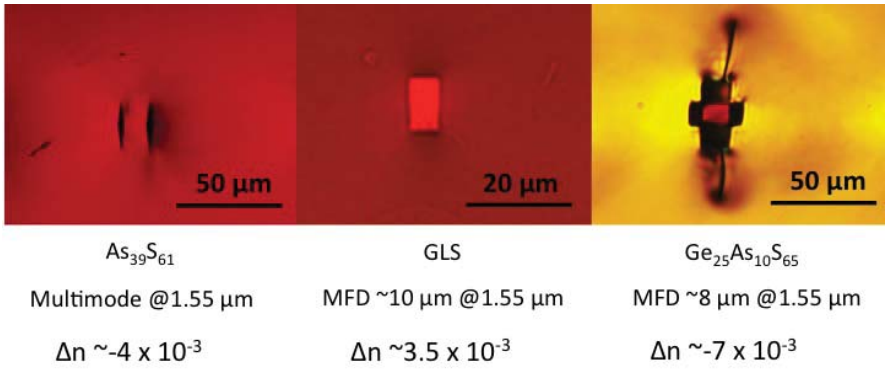

Fig. 3. Bright-field microscope image, mode field diameter and estimated refractive index contrast of (left to right): $As_{39}S_{61}$, GLS and $Ge_{25}As_{10}S_{65}$.

Four kinds of waveguides were formed (P1, P2, N1 and N3). For glasses such as $As_{39}S_{61}$, $Ge_{15}Sb_{20}S_{65}$ and $Ge_{11.5}As_{24}S_{64.5}$ stress waveguides (N1) were created as the superposition of several modification led stress induced fractures in the glass. For the same reason, no single mode waveguide could be fabricated for 1550 nm guidance (see Fig. 3). However, bigger waveguide structures were characterised at longer wavelengths in $As_{39}S_{61}$, resulting in mode field diameters around 33 μm when injecting light at 3.39 μm and an estimated refractive index change of -4×10^{-3}. The cross-sectional shape obtained for $Ge_{25}As_{10}S_{65}$ was very similar to the previous case yet the thermal expansion coefficient of this glass is lower, which allows for the superposition of multiple tracks (N2) without suffering from catastrophic damage. Some fractures can be observed on Fig. 3c, but the structure still guided light. The refractive index contrast obtained for this glass was the largest of any of the glasses with negative modification (-7×10^{-3}), leading to the smallest MFD. The same order of magnitude (but opposite sign) refractive index contrast was

Optical Materials EXPRESS

obtained for 75(GeS_2)-15(Ga_2S_3)-10(CsCl).

While comparable refractive index contrast to those reported in the literature was also obtained for GLS [13, 58, 62], for other chalcogenides such as the Ge-As-S family (i.e. $Ge_{25}As_{10}S_{65}$), the refractive index contrast was around 10× the value reported by *Damico et al.* in their work based on $Ge_{15}As_{15}S_{70}$ [44]. Refractive index contrasts in the order of mid 10^{-3} are needed to keep the modes tightly confined inside the waveguide structure and to be able to design bends in the waveguides without major losses.

4.2. Fluorides

Crystals based on two atomic elements by the ionic bond between fluorine and an alkaline earth metal (group IIA) have a low refractive index and show remarkably high transparency from the visible to long infrared wavelengths. For these reasons. some of these crystals such as BaF_2 and CaF_2 are commonly used for the fabrication of MIR lenses. Being crystalline materials the interaction with femtosecond laser pulses for the fabrication of waveguides in the thermal regime is far from ideal as the modifications tend to show a pearl chain structure [77], making it impossible to generate a low-loss waveguide. Here, the fabrication of waveguides in CaF_2 was investigated with no successful waveguiding results (see Fig. 4b).

In the case of fluorides from the IZSBGC family, the problem was not the nonlinearity but a series of positive and negative substructures generated when trying to scale up the waveguide size by increasing the fluence in the thermal fabrication process. At low pulse energies, the waveguides show a close-to-homogenous refractive index profile (although low refractive index contrast 9×10^{-4}), but this configuration is not maintained when increasing the pulse energy. A solution for this is to overlap multiple tracks in a circular configuration around a central modification in order to create larger waveguide structures. However, this approach did not work as expected for IZSBGC glasses as the refractive index contrast was too small, thus the mode confinement was weak and the light leaked into the bulk material, making the waveguides highly lossy. The refractive index change values obtained during these experiments for fluoride glasses agree with those obtained previously in the literature for ZBLAN [80]. *Lancaster et al.* reported a refractive index contrast of the same order of magnitude (but opposite in sign) for their Tm:ZBLAN waveguide lasers [80]. Fig. 4 shows the best results obtained for fluoride materials.

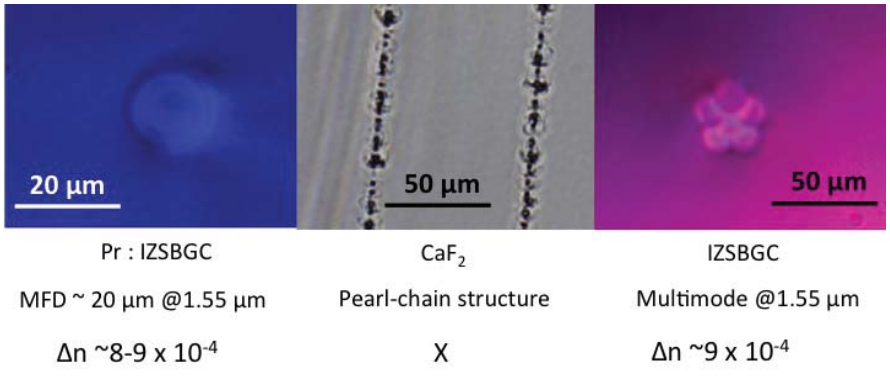

Fig. 4. Some examples obtained for 3 fluoride materials (left to right): Pr : IZSBGC, CaF_2 and IZSBGC. Bright-field microscope image, mode field diameter and estimated refractive index contrast.

Optical Materials EXPRESS

4.3. Germanate glass

When the shape of the modification is close to a circle (either circular or oval) and the sign of the refractive index of the modified region is negative, the best waveguide format is to surround an unmodified region of material by a superposition of negative modifications to form a depressed cladding. The mode will then travel though the unmodified region, while the depressed cladding arrangement will confine the light inside the structure. One of the main benefits of this technique is that it is extremely easy to scale with wavelengths, by controlling the size of the waveguide. This waveguide composition has been successfully shown in fluorozirconate glass materials such as ZBLAN [14] with low propagation losses in the MIR. When fabricating interferometric devices, the small refractive index contrast ($\sim 10^{-3}$, low confinement) obtained in ZBLAN would result in large bend losses or extremely long waveguides, which would consequently mean large overall losses. Materials like Schott IRG-2 can manifest in a refractive index contrast up to 10× larger than ZBLAN, which leads to a higher mode confinement and, therefore, to low bend losses. For the fabrication of depressed cladding waveguides (N3) the best results in the thermal regime were obtained for IRG-2 with a refractive index contrast of around -5×10^{-3} and a mode field diameter of 8.3 μm when injecting light at 1550 nm. One of the benefits of IRG-2 and its moderate/large refractive index contrast is the ease of scaling the waveguide core size for single-mode propagation at different wavelengths. Fig. 5 shows the best waveguide result obtained for IRG-2 germanate glass.

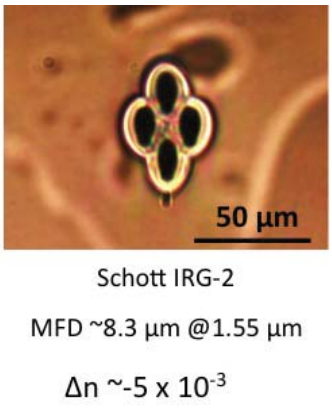

Fig. 5. Bright-field microscope image, mode field diameter and estimated refractive index contrast of IRG2.

5. Discusion

One of the main challenges for astrophotonic devices is the need for low intrinsic losses (< 1 dB/cm), meaning that the glass absorption will always need to be below that value for these devices to be efficient. Any extra loss would mean that less photons would arrive at the detector after travelling through the instrument. This problem can be mitigated with one or more of the following solutions: using a larger telescope, lower readout noise cameras and longer integration times; all of them increase the cost of the experiment and/or reduce the efficiency of the system. Access to larger telescopes is expensive and very limited unless the instrument has already been tested in smaller telescopes with high success. Increasing the camera's integration time not only reduces the efficiency of the already expensive telescope time, but can also lead to other problems such as an increase in the noise level, which can mask interesting results. This problem can be addressed using low readout noise cameras/detectors which may not be accessible (and the price

Optical Materials EXPRESS

increases exponentially as the readout noise decreases). All these solutions are therefore either expensive, inefficient or both, meaning that special care needs to be taken on the reduction of glass absorption and waveguide intrinsic losses.

Depending on the sign and shape of the refractive index modification obtained when exposing mid-infrared materials to femtosecond laser irradiation, different approaches can be used when creating waveguides. When the refractive index sign of a single modification is negative, the guided mode will travel through unmodified material surrounded by several negative tracks. When the refractive index change is positive, the waveguide can be formed from a single modification or an overlap of several depending on the shape of the single track cross-section. Table 4 summarises the results obtained for each glass including preferred geometry, the horizontal MFD and the induced refractive index contrast.

Table 4. Summary of the results obtained for each glass including the preferred waveguide geometry, the horizontal mode field diameter (MFD) and the refractive index contrast.

Glass name	Preferred Geometry	MFD (1.55 μm)	Δn
$As_{39}S_{61}$	N1	Multimode	-4×10^{-3}
75(GeS_2)-15(Ga_2S_3)-10(CsCl)	P1	8 μm	7×10^{-3}
Pr : IZSBGC	P1	20 μm	$8 - 9 \times 10^{-4}$
IZSBGC	P3	Multimode	9×10^{-4}
La : IZSBGC	P1	22 μm	8×10^{-4}
$Ge_{15}Sb_{20}S_{65}$	N1	11 μm	-3×10^{-3}
$Ge_{11.5}As_{24}S_{64.5}$	N1	10 μm	-3.5×10^{-3}
$Ge_{25}As_{10}S_{65}$	N3	8 μm	-7×10^{-3}
GLS	P2	10 μm	3.5×10^{-3}
IRG-2	N2	8.3 μm	-5×10^{-3}

It is important to note that low refractive index materials (i.e. fluorides) that a priori seem ideal for the fabrication of low-loss waveguides, due to their lower Fresnel losses, tend to exhibit a refractive index contrast ($\sim 10^{-4}$) that is too low for tight mode confinement. This results in large bend-losses associated with light leaking out of the waveguide structure. Other materials like chalcogenide glasses possess a larger refractive index (usually > 2), but they also have larger nonlinearities. As the focused beam travels through the glass it suffers from aberrations, which affects the focal volume shape and is intensity dependent. A simple way to create bigger structures that do not suffer large aberrations is the superposition of small modifications to form waveguides. One of the benefits of the superposition approach is the ability to arbitrarily scale and choose the shape of the waveguides depending on the application needs. The best three chalcogenides to fabricate waveguides using the superposition of multiple tracks under the optimized exposure conditions were GLS, 75(GeS_2)-15(Ga_2S_3)-10(CsCl) and $Ge_{25}As_{10}S_{65}$. For the latter one, the addition of the right amount of Germanium to the As-S family of glasses helps tailor the mechanical properties and refractive index of the modification.

Finally, one glass that offers easy scalability while having an intermediate refractive index (~1.89) and nonlinearity is Schott IRG-2. Under the tested conditions, this germanate glass exhibited oval-shaped highly-negative refractive index modifications ($\sim -5 \times 10^{-3}$) that allowed for the fabrication of depressed cladding waveguides in a relatively simple manner.

For all the tested materials, the easiest way to generate single-mode waveguides in the L' band was the overlap of individual modifications to create a larger structure, whether it was by generating a depressed cladding waveguide or a positive refractive index core surrounded by unmodified bulk glass. The superposition of individual modification tracks adds the possibility of tailoring the glass refractive index modification and the size of the guided mode.

The characterisation of the propagation losses falls out of the scope of this paper and will be

Optical Materials EXPRESS

reported in a follow up manuscript.

6. Conclusion

This paper reports a study of laser writing results and outlines the best strategy for successful writing of waveguides and discusses the role of the optical material properties on this process. We believe the waveguide refractive index contrast results obtained for some of the glasses explored in this manuscript show evidence that low-loss astrophotonic devices for the L'-band ($3.5 - 4.1\mu$m) will be possible in the next few years. These glasses include chalcogenides such as GLS, $Ge_{25}As_{10}S_{65}$ and $75(GeS_2)$-$15(Ga_2S_3)$-10(CsCl), and germanate glasses such as IRG-2. Furthermore, the transparency of some of these glasses, such as $75(GeS_2)$-$15(Ga_2S_3)$-10(CsCl) and $Ge_{15}Sb_{20}S_{65}$, expands up to the N-band, an atmospheric transmission window centered at 10 μm. The N-band is of special interest in the study of molecular clouds and protostars, allowing advanced photonic instrumentation to be constructed for these, and a handful of other astronomical themes based in this waveband.

Funding

This research was supported by the Australian Research Council Centre of Excellence for Ultrahigh bandwidth Devices for Optical Systems (project number CE110001018) and was performed in part at the Optofab node of the Australian National Fabrication Facility using Commonwealth and NSW and SA State Government funding. S. Gross acknowledges funding by a Macquarie University Research Fellowship.